This article was downloaded by: [Institute Of Atmospheric Physics]
On: 09 December 2014, At: 15:34
Publisher: Taylor & Francis
Informa Ltd Registered in England and Wales Registered Number: 1072954 Registered office: Mortimer House, 37-41 Mortimer Street, London W1T 3JH, UK

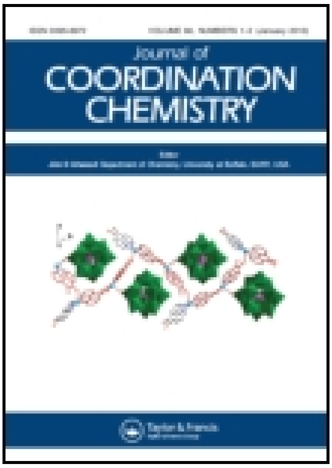

CrossMark

Click for updates

Journal of Coordination Chemistry

Publication details, including instructions for authors and subscription information:
http://www.tandfonline.com/loi/gcoo20

# α-Keggin tungstogermanate-supported transition metal complexes: hydrothermal synthesis, characterization, and magnetism of $Cu_2(phen)_4(GeW_{12}O_{40})$ and $[Ni_2(bpy)_4(H_2O)_2(GeW_{12}O_{40})]\cdot 2H_2O$

Bi-Song Zhang[a], Chang-Sheng Wu[a], Jian-Ping Qiu[a], Yun-Xia Li[a] & Zhen-Xiang Liu[a]

[a] Institute of Materia Medica, College of Pharmaceutics and Material Engineering, Jinhua Polytechnic, Jinhua, PR China

Accepted author version posted online: 19 Mar 2014.Published online: 10 Apr 2014.

To cite this article: Bi-Song Zhang, Chang-Sheng Wu, Jian-Ping Qiu, Yun-Xia Li & Zhen-Xiang Liu (2014) α-Keggin tungstogermanate-supported transition metal complexes: hydrothermal synthesis, characterization, and magnetism of $Cu_2(phen)_4(GeW_{12}O_{40})$ and $[Ni_2(bpy)_4(H_2O)_2(GeW_{12}O_{40})]\cdot 2H_2O$, Journal of Coordination Chemistry, 67:5, 787-796, DOI: 10.1080/00958972.2014.904855

To link to this article: http://dx.doi.org/10.1080/00958972.2014.904855

PLEASE SCROLL DOWN FOR ARTICLE

Taylor & Francis makes every effort to ensure the accuracy of all the information (the “Content”) contained in the publications on our platform. However, Taylor & Francis, our agents, and our licensors make no representations or warranties whatsoever as to the accuracy, completeness, or suitability for any purpose of the Content. Any opinions and views expressed in this publication are the opinions and views of the authors, and are not the views of or endorsed by Taylor & Francis. The accuracy of the Content should not be relied upon and should be independently verified with primary sources of information. Taylor and Francis shall not be liable for any losses, actions, claims, proceedings, demands, costs, expenses, damages, and other liabilities whatsoever or howsoever caused arising directly or indirectly in connection with, in relation to or arising out of the use of the Content.

*Journal of Coordination Chemistry*, 2014
Vol. 67, No. 5, 787–796, http://dx.doi.org/10.1080/00958972.2014.904855

# α-Keggin tungstogermanate-supported transition metal complexes: hydrothermal synthesis, characterization, and magnetism of $Cu_2(phen)_4(GeW_{12}O_{40})$ and $[Ni_2(bpy)_4(H_2O)_2(GeW_{12}O_{40})]\cdot 2H_2O$

BI-SONG ZHANG*, CHANG-SHENG WU, JIAN-PING QIU, YUN-XIA LI and ZHEN-XIANG LIU

Institute of Materia Medica, College of Pharmaceutics and Material Engineering, Jinhua Polytechnic, Jinhua, PR China

(*Received 17 August 2013; accepted 26 February 2014*)

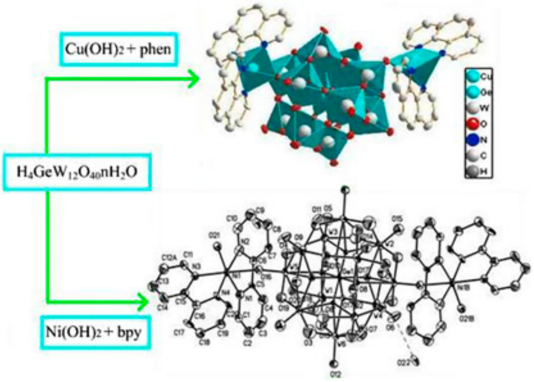

Two new α-Keggin polyoxometalates, $[Cu_2(phen)_4(GeW_{12}O_{40})]$ (**1**) and $[Ni_2(bpy)_4(H_2O)_2(GeW_{12}O_{40})]\cdot 2H_2O$ (**2**) (phen = 1,10-phenanthroline, bpy = 2,2′-bipyridine), have been hydrothermally synthesized and characterized by elemental analysis, IR, TG, single-crystal X-ray diffraction, and magnetic properties. Compound **1** crystallizes in the monoclinic system, space group *P2(1)/c*, and **1** is assembled into two-dimensional (2-D) layers parallel to (1 0 1) based on the adjacent phen $\pi\cdots\pi$ stacking interactions (3.788(8) Å). Variable temperature magnetic measurements show ferromagnetic behavior from 300 to 2 K. Compound **2** crystallizes in the triclinic system, space group *P-1*, and **2** is assembled into 2-D layers parallel to (1 0 1) based on the adjacent bpy $\pi\cdots\pi$ stacking interactions (3.07 Å). Variable temperature magnetic measurements show a weak ferromagnetic behavior from 300 to 26 K followed by antiferromagnetic behavior below 26 K.

*Keywords*: Transition metal complexes; α-Keggin polyoxometalates; Tungstogermanates; Crystal structure; Magnetic property

---

*Corresponding author. Email: zbs_jy@163.com

## 1. Introduction

Polyoxometalates (POMs) have been known for more than 200 years, with sustained attention due to their intriguing structures and potential applications in medicine, materials science, adsorption, catalysis, separation, electric conductivity, and magnetism [1–3]. Decoration of polyoxoanions with various organic and transition metal complexes [4–6], which may enrich the framework, leads to new applications in many fields. Much work has been attracted to construction of new organic–inorganic complexes based on POMs and transition metal complexes [7–12]. Keggin-type POMs can coordinate to transition metals using their terminal or bridging oxygens [13–16].

Our group is interested in applications of Keggin-type heteropolyoxotungstate-supported inorganic–organic hybrids and exploiting its linking propensity with metal ions to obtain extended structures and new materials [17–29]. Recently, we began to use $H_4GeW_{12}O_{40}$ as a ligand to synthesize POM-supported transition metal complexes, and have succeeded in connecting this versatile building unit $[GeW_{12}O_{40}]^{4-}$ to complete germanium–tungsten cluster-supported transition metal complexes, $[Cu_2(phen)_4(GeW_{12}O_{40})]$ (**1**) and $[Ni_2(bpy)_4(H_2O)_2(GeW_{12}O_{40})]\cdot 2H_2O$ (**2**). To the best of our knowledge, it has been rarely reported that α-Keggin heteropolyotungstates simultaneously support transition metal complex moieties that display different geometries. There are two crystallographically independent copper sites with two different coordination environments in the complex reported below.

## 2. Experimental

### 2.1. *Materials and physical methods*

All chemicals purchased were of reagent grade as received from commercial sources and used without purification. $H_4GeW_{12}O_{40}\cdot nH_2O$ was prepared according to a literature method [30]. Distilled water was used in the reaction. Elemental analyses were performed on a Perkin-Elmer 2400 CHN Elemental Analyzer (C, H, and N) and on a Leaman inductively coupled plasma spectrometer (Cu and Ni). IR spectra (KBr pellets) were recorded from 400 to 4000 $cm^{-1}$ on an Alpha Centauri FTIR spectrophotometer. TG/DTA measurements were performed under a flow of nitrogen from room temperature to 800 °C at a heating rate of 10 °C/min using a Seiko Exstar 6000 TG/DTA 6300 apparatus. Single crystal diffraction data were collected on a Rigaku R-Axis Rapid IP X-ray diffractometer. Temperature-dependent magnetic susceptibilities were determined with a Quantum Design SQUID magnetometer (Quantum Design Model MPMS-7) from 2 to 300 K with an applied field of 1000 G.

### 2.2. *Synthesis of $[Cu_2(phen)_4(GeW_{12}O_{40})]$ (1)*

$CuSO_4\cdot 5H_2O$ (0.245 g, 1.00 mM) was dissolved in water and then 1 M NaOH solution was added. $Cu(OH)_2$ was obtained by filtration, which was then washed with distilled water five times. The freshly prepared $Cu(OH)_2$, phen·$H_2O$ (0.200 g, 1.00 mM) $H_4GeW_{12}O_{40}\cdot nH_2O$ (3.110 g, 1.00 mM), and $CH_3OH/H_2O$ (v/v = 1 : 2, 15 mL) were mixed and stirred for 2 h. The resulting blue suspension was heated in a 23 mL Teflon-lined stainless steel autoclave at 433 K for 100 h. After the autoclave was cooled to room temperature over 12 h, blue block single crystals of **1** were obtained and then washed with distilled water and finally dried in air (yield: 33.98% based on the initial phen·$H_2O$ input). $C_{48}H_{32}Cu_2GeN_8O_{40}W_{12}$ (3766.69): Calcd C 15.29, H 0.85, N 2.97, Cu 3.37%; Found: C 15.24, H 0.93, N 2.95, Cu 3.35%. IR ($cm^{-1}$, KBr): 3426m, 3068m, 1625m, 1564m, 1519s, 1494s, 1429s, 968s, 885s, 806m, 779s.

### 2.3. *Synthesis of* $[Ni_2(bpy)_4(H_2O)_2(GeW_{12}O_{40})]\cdot 2H_2O$ *(2)*

The synthetic procedure analogous to **1** was carried out except 0.6265 g 1 mM $NiSO_4\cdot 6H_2O$ instead of $CuSO_4\cdot 5H_2O$ and 0.1565 g 1 mM 2,2′-bpy instead of phen·$H_2O$, $H_4GeW_{12}O_{40}\cdot nH_2O$ (1.555 g, 0.50 mM); purple block single crystals of **2** were obtained and then washed with distilled water and finally dried in air (yield: 24.96% based on the initial 2,2′-bpy input). $C_{40}H_{40}GeN_8Ni_2O_{44}W_{12}$ (3733.01): Calcd C 12.86, H 1.07, N 3.00, Ni 3.14%; Found: C 12.79, H 1.13, N 2.97, Ni 3.13%. IR ($cm^{-1}$, KBr): 3450m, 3100w, 1600s, 1440s, 960s, 879s, 829m, 783s, 733m, 463s.

### 2.4. *X-ray crystallography*

Suitable single crystals of **1** and **2** were selected under a polarizing microscope and fixed with epoxy cement on fine glass fibers. Compounds **1** and **2** were mounted on a Rigaku R-Axis Rapid IP X-ray diffractometer with graphite-monochromated Mo-$K\alpha$ radiation ($\lambda = 0.71073$ Å) for cell determination and subsequent data collection. Data were collected from $3.02° \le \theta \le 27.48°$. All the data were corrected for *Lp* and empirical absorption effects. The structures were solved using direct methods. SHELXS-97 [31] and SHELXL-97 [31] were used for structure solution and refinement. Subsequent difference Fourier syntheses enabled all non-hydrogen atoms to be located. After several cycles of refinement, hydrogens bonded to carbon were added in calculated positions and hydrogens of $H_2O$ were derived from difference Fourier syntheses. Finally, all non-hydrogen atoms were refined with anisotropic displacement parameters by full-matrix least-squares technique and hydrogens with isotropic displacement parameters. The crystal data, intensity collection, and details of structure refinement are summarized in table 1. Selected interatomic distances, bond angles, and hydrogen bond parameters are given in tables S1–S3 (see online supplemental material at http://dx.doi.org/10.1080/00958972.2014.904855).

## 3. Results and discussion

### 3.1. *Syntheses*

Wang and Niu reported that, under hydrothermal conditions, reaction of $CuCl_2\cdot 2H_2O$, $H_4GeW_{12}O_{40}\cdot nH_2O$, and phen (pH of the mixture was carefully adjusted to 8.27 with 4 M NaOH), in an aqueous solution with the molar ratio of 8.0 : 1.0 : 40 at 160 °C, produced a one-dimensional (1-D) POM-based complex $\{[Cu^{I}(en)_2(H_2O)]_2\{GeW_{12}O_{40}[Cu^{II}(en)_2]\}\cdot 2.5H_2O\}_n$ [14]. Meng and Chen also reported under hydrothermal conditions, reaction of $CuSO_4\cdot 5H_2O$, $H_4SiW_{12}O_{40}\cdot nH_2O$ and phen (pH of the mixture was carefully adjusted to 2.8 with 4 M HCl), in an aqueous solution with the molar ratio of 2.5 : 1.0 : 3.5 at 160 °C, produced metal-oxo cluster-supported transition metal complexes $[\{Cu(phen)_2\}_2SiW_{12}O_{40}]$ [9]. We found that in the presence of phen(bpy), hydrothermal reactions of $M(OH)_2$ and

Table 1. Crystal data and structure refinement parameters for **1** and **2**.[a]

| | **1** | **2** |
|---|---|---|
| Empirical formula | $C_{48}H_{32}Cu_2GeN_8O_{40}W_{12}$ | $C_{40}H_{40}GeN_8Ni_2O_{44}W_{12}$ |
| Formula mass | 3766.69 | 3733.01 |
| Temperature (K) | 293(2) | 293(2) |
| Wavelength (Å) | 0.71073 | 0.71073 |
| Crystal system | Monoclinic | Triclinic |
| Space group | *P2(1)/c* | *P-1* |
| $a$ (Å) | 26.049(5) | 10.484(2) |
| $b$ (Å) | 12.031(2) | 13.399(3) |
| $c$ (Å) | 23.351(5) | 13.605(3) |
| $\alpha$ (°) | 90 | 70.20(3) |
| $\beta$ (°) | 113.73(3) | 68.77(3) |
| $\gamma$ (°) | 90 | 73.95(3) |
| Volume (Å$^3$) | 6699(2) | 1650.1(6) |
| $Z$ | 4 | 1 |
| $D_{\text{Calcd}}$ (g cm$^{-3}$) | 3.735 | 3.757 |
| $F(0\,0\,0)$ | 6696 | 1664 |
| Reflections collected | 50,824 | 12,609 |
| Reflections unique ($R_{\text{int}}$) | 11,751 (0.1810) | 5696 (0.1192) |
| $\mu$ (mm$^{-1}$) | 21.672 | 21.925 |
| $\theta$ range (°) | 3.02–25.00 | 3.06–25.00 |
| $R_1$, $wR_2$ [$I \geq 2\sigma(I)$][a] | 0.0592, 0.1313 | 0.0928, 0.2016 |
| $R_1$, $wR_2$ (all data)[a] | 0.0679, 0.1369 | 0.1125, 0.2124 |
| Goodness of fit on $F^2$ | 1.086 | 1.164 |
| Extinction coefficient | 0.000149(16) | 0.00073(10) |
| $\delta\rho_{\max}$, $\delta\rho_{\min}$ (e Å$^{-3}$) | 5.051, −2.494 | 3.267, −2.775 |

[a] $R_1 = \Sigma(|F_o| - |F_c|)/\Sigma|F_o|$, $wR_2 = [\Sigma w(F_o^2 - F_c^2)^2/\Sigma w(F_o^2)^2]^{1/2}$, and $w = [\sigma^2(F_o^2) + (aP)^2 + bP]^{-1}$, where $P = (F_o^2 + 2F_c^2)/3$.

$H_4GeW_{12}O_{40}{\cdot}nH_2O$ in mixed solvents such as $CH_3OH–H_2O$ (v/v = 1 : 2) in the molar ratio of 2.0 : 4.0 : 1.0 (M: organic ligand: POM) at 160 °C yielded **1** and **2**, and the reactions can be expressed as follows:

$$2\mathrm{Cu(OH)_2} + \mathrm{H_4GeW_{12}O_{40}} \cdot n\mathrm{H_2O} + 4\mathrm{phen} \rightarrow [\mathrm{Cu_2(phen)_4(GeW_{12}O_{40})}](\mathbf{1}) + (n+4)\mathrm{H_2O}$$

$$2\mathrm{Ni(OH)_2} + \mathrm{H_4GeW_{12}O_{40}} \cdot n\mathrm{H_2O} + 4\mathrm{bpy} \rightarrow [\mathrm{Ni_2(bpy)_4(H_2O)_2(GeW_{12}O_{40})}] \cdot 2\mathrm{H_2O}\ (\mathbf{2}) + n\mathrm{H_2O}$$

A series of synthesis experiments indicate the optimal reaction molar ratio of 2.0 : 4.0 : 1.0 (M : organic ligand : POM) and substitution of mixed solvents such as $CH_3OH–H_2O$ (v/v = 1 : 2) for water. The crystals are stable in air and insoluble in water and methanol.

### 3.2. *Description of crystal structures*

Complex **1** consists of two $[Cu(phen)_2]^{2+}$ cations and one $[GeW_{12}O_{40}]^{4-}$ [figure 1(a)]. The heteropolyanion $[GeW_{12}O_{40}]^{4-}$ exhibits the well-known α-Keggin structure, which consists of 12 $WO_6$ octahedra and one $GeO_4$ tetrahedron. The central $GeO_4$ tetrahedron shares its oxygens with four $\{W_3O_{13}\}$ groups, each of which is made up of three edge-sharing $WO_6$

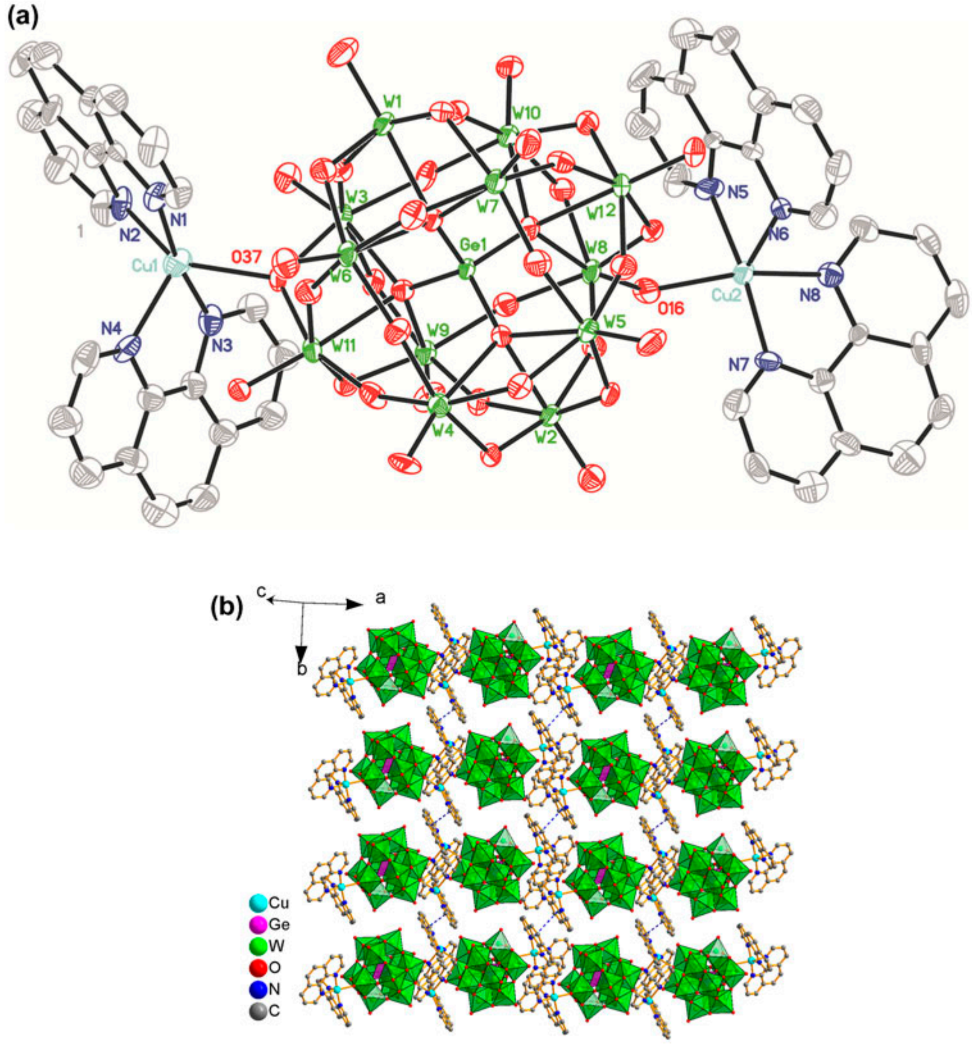

Figure 1. (a) Molecular structure of **1** together with atom numbering scheme and thermal ellipsoids drawn at 45% probability level and (b) 2-D layer built from 1-D chains connected by $\pi\cdots\pi$ interactions (dashed lines).

octahedra. $W_3O_{13}$ subunits are joined by corner-sharing oxygens, which can be divided into four groups according to their coordination in $[GeW_{12}O_{40}]^{4-}$: $O_t$ terminal oxygens connect to one W, $O_b$ share corners between two $W_3O_{13}$ units, $O_c$ connect edge-sharing $WO_6$ octahedra in the same $W_3O_{13}$ unit, and $O_a$ connect the Ge and three W. The Ge–O distances are 1.722(11)−1.743(9) Å, while the O–Ge–O angles vary from 108.9(4)° to 110.4(5)°. Relevant W–O bond distances in the anion can be classified into three groups: W–$O_t$ 1.687(9)–1.755(11) Å, W–$O_{b,c}$ 1.854(8)–1.977(9) Å, and W–$O_a$ 2.255(11)–2.322(8) Å, indicating that the polyanion maintains the basic Keggin structure. However, compared with the averages, W(8)–$O_t$(16) (1.755 Å) and W(3,11)–$O_c$(37) (1.952 Å, 2.010 Å) bonds are lengthened (table S1), caused by coordination of copper to surface oxygens of the polyanion.

Complex **1** has a surface bridging and a terminal oxygen of the polyoxoanion coordinated to two $[Cu(phen)_2]^{2+}$ cations. There are two distinct copper(II) coordination geometries. As illustrated in figure 1(a), Cu(1) is coordinated by four nitrogens from two phen and one bridge-oxygen ($O_c37$) of the α-Keggin unit. The apical site is occupied by two nitrogens. The basal positions are occupied by two nitrogens from phen and oxygen from the polyoxotungstate. The Cu(1)–O(37) distance is 2.274(9) Å, while Cu(1)–N bond lengths are in the range of 1.958(16)–2.168(13) Å. The coordination sphere of Cu(1) is best described from the $\tau$ value of 0.41 ($\tau = 0$ for a perfect square pyramid, $\tau = 1$ for a perfect trigonal bipyramid) [17], which indicates that coordination polyhedron of Cu(1) is a highly distorted trigonal bipyramid. Cu(2) exhibits a similar coordination environment. The Cu(2)–O(16) bond distance is 2.053(10) Å, while the Cu(2)–N distances vary from 1.975(13) to 2.218(14) Å. Cu(2) is in a square pyramidal environment ($\tau$Cu(2) = 0.13). The overall structure is very similar with that of the literature [9] except the central atom.

Molecules of **1** are joined by $\pi$–$\pi$ stacking interactions involving phen and hydrogen bonding between hydrogens on phen and oxygen of polyanions, with C–H…O distances of 2.9264–3.4663 Å, the closest contact between adjacent aromatic rings is 3.43(5) Å. Thus, the structure forms a 1-D, toothed, chain-like arrangement via weak $\pi$–$\pi$ stacking [figure 1(b)]. Hydrogen bonds link the chains to give an infinite 2-D planar structure [figure 1(b)]. The extensive hydrogen bonding array contributes to the stability of the structure.

$[Ni_2(bpy)_4(H_2O)_2(GeW_{12}O_{40})]\cdot 2H_2O$ (**2**). The crystal structure of **2** is similar to **1**, but with differences. First, **1** crystallizes in the monoclinic system, space group *P2(1)/c*, and **2** crystallizes in the triclinic system, space group *P-1*. Second, **2** consists of two $[Ni(bpy)_2(H_2O)]^{2+}$ cations, one $[GeW_{12}O_{40}]^{4-}$ and two crystal waters [figure 2(a)]. The heteropolyanion $[GeW_{12}O_{40}]^{4-}$ also exhibits the well-known α-Keggin type structure, with germanium in the center of the polyanion and the four oxygens of $GeO_4$ tetrahedron are disordered. Ge is surrounded by a cube of eight oxygens (O(8) and $O(8)^i$, O(17) and $O(17)^i$, O(8′) and $O(8')^i$, and O(17′) and $O(17')^i$, i: $-x$, $-y$, $-z+1$), and each oxygen has two equal sites half-occupied, located in the center of the host cage with Ge–O average distance 1.68 (3) Å and O–Ge–O angles from 107.6(16)° to 110.2(16)°. Third, **2** has two terminal oxygens on the surface of the polyoxoanion coordinated to two $[Ni(bpy)_2(H_2O)]^{2+}$ cations. There are two nickel(II) coordination geometries. As illustrated in figure 2(a), Ni(1) is coordinated by four nitrogens from two bpy, one terminal oxygen ($O_t16$) of the α-Keggin unit, and one water oxygen to complete a $NiN_4O_2$ octahedral geometry. Fourth, due to the presence of coordinated water and lattice water, molecules of **2** are joined by $\pi$–$\pi$ stacking interactions involving bpy groups and extensive hydrogen bonding between the water ligand and lattice water [figure 2(b)], with O–H…O distances of 2.714–2.977 Å, the closest contact between adjacent aromatic rings is 3.07(4) Å. Literature [8, 9, 18–29] suggests that the central heteroatom of different complexes is influenced by their surroundings, such as coordination bonds, hydrogen bonds, and weak interactions; when they are symmetrical, the central heteroatom would be disordered.

### 3.3. *Infrared spectrum*

In the IR spectrum (figures S1 and S3) of **1** and **2**, there are four characteristic asymmetric vibrations resulting from polyanions with the Keggin structure, $\nu_{as}(W–O_t)$, $\nu_{as}(W–O_b)$, $\nu_{as}(W–O_c)$, and $\nu_{as}(Ge–O_a)$ at 968, 885, 779, and 806 $cm^{-1}$ for **1**, 960, 879, 783, and 829 $cm^{-1}$ for **2**, respectively. Comparing the IR spectrum of **1** and **2** with that of

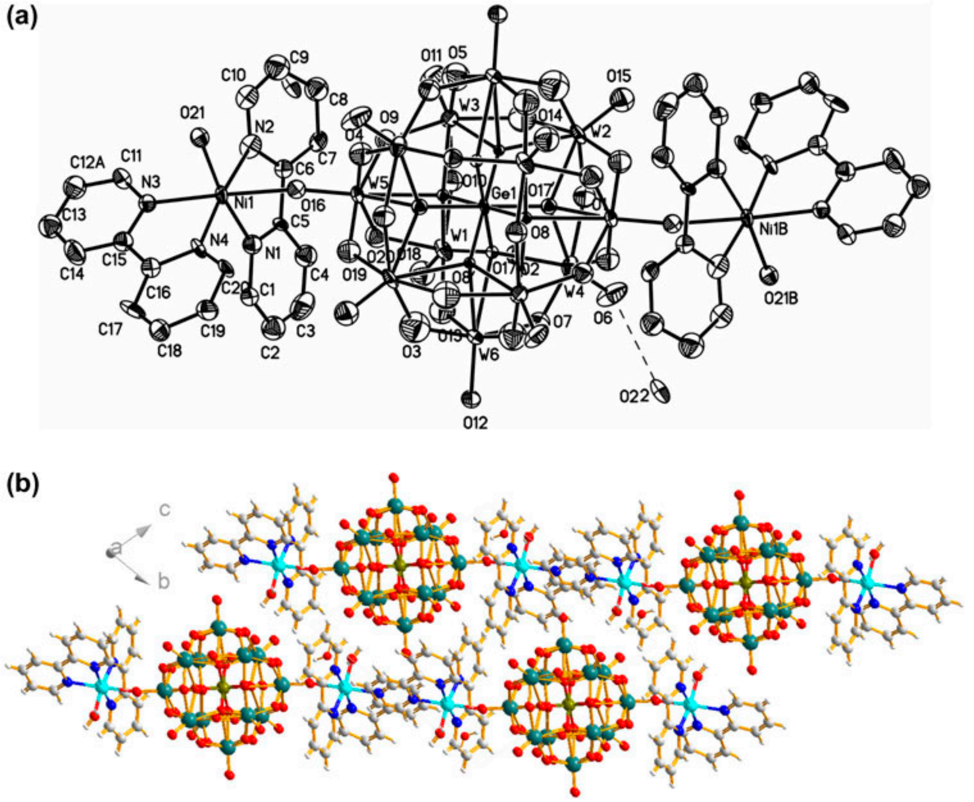

Figure 2. (a) Molecular structure of **2** together with atom numbering scheme and thermal ellipsoids drawn at 45% probability level and (b) layered structure of **2** joined by $\pi$–$\pi$ stacking interactions.

$H_4GeW_{12}O_{40}$ (figure S5), the W–$O_t$ stretch shifted from 983 to 968, 960 $cm^{-1}$, the Ge–$O_a$, W–$O_b$, and W–$O_c$ vibrations shifted from 821 to 806 and 829 $cm^{-1}$, 881 to 885 and 879 $cm^{-1}$, and 763 to 779 and 783 $cm^{-1}$ [32], indicating that $[GeW_{12}O_{40}]^{4-}$ was affected by the surrounding metal cations. This is in agreement with the single-crystal X-ray diffraction analysis. Vibrations at 3068 and 3100, 1100–1600 $cm^{-1}$ are, respectively, assigned to $\nu_{as}$(C–H) and $\nu_{as}$(C–N) of phen and bpy of **1** and **2**; **2** displays a broad absorption at 3200–3600 $cm^{-1}$ due to stretch of $H_2O$.

### 3.4. *Thermal analyses*

The TG/DTA curves of **1** and **2** are provided in figures S2 and S4 (Supplementary material). For **1**, the TG curve exhibits continuous weight loss of 21.20% from 50 to 600 °C, ascribed to release of phen (Calcd 19.11%) and decomposition of POMs (Calcd 2.09%). For **2**, the first weight loss of 2.11% at 20–197 °C corresponds to loss of water, agreeing with the calculated value of 1.93% for four $H_2O$ per empirical formula unit. The second and third step weight loss of 19.17% is ascribed to release of bpy (Calcd 16.72%) and decomposition of POMs (Calcd 2.45%).

### 3.5. *Magnetic properties*

Magnetic susceptibility data were recorded for **1** and **2** from 300 to 2 K with an applied field of 1000 Oe. The magnetic behaviors in the form of $\chi_m$ and $\chi_m T$ *versus T* plots are depicted in figure 3. The $\chi_m T$ value for 1 [figure 3(a)] increases linearly from 0.58 cm$^3$ M$^{-1}$ K at 300 K to a maximum of 0.85 cm$^3$ M$^{-1}$ K at 7 K, followed by a slight decrease to 0.84 cm$^3$ M$^{-1}$ K at 2 K. At room temperature, the $\chi_m T$ value of 0.58 cm$^3$ M$^{-1}$ K is larger than the spin-only value of 0.37 cm$^3$ M$^{-1}$ K for high-spin Cu(II) ($s$ = 1/2), indicating a larger orbital contribution arising from the $^2T_2$ and $^2E$ ground term in tetrahedral ligand fields. With temperature decrease, the $\chi_m T$ values rise, reaching 0.85 cm$^3$ K M$^{-1}$ at 7 K, which is typical of an overall ferromagnetic interaction between Cu(II) ions. Based on the spin Hamiltonian $H = -2JS_1S_2$, the following equation was used to fit the magnetic susceptibility data (1):

$$\chi_M = \frac{(2N\beta^2 g^2)}{3kT}\left[1 + \frac{1}{3}\exp(-2J/kT)\right]^{-1} \tag{1}$$

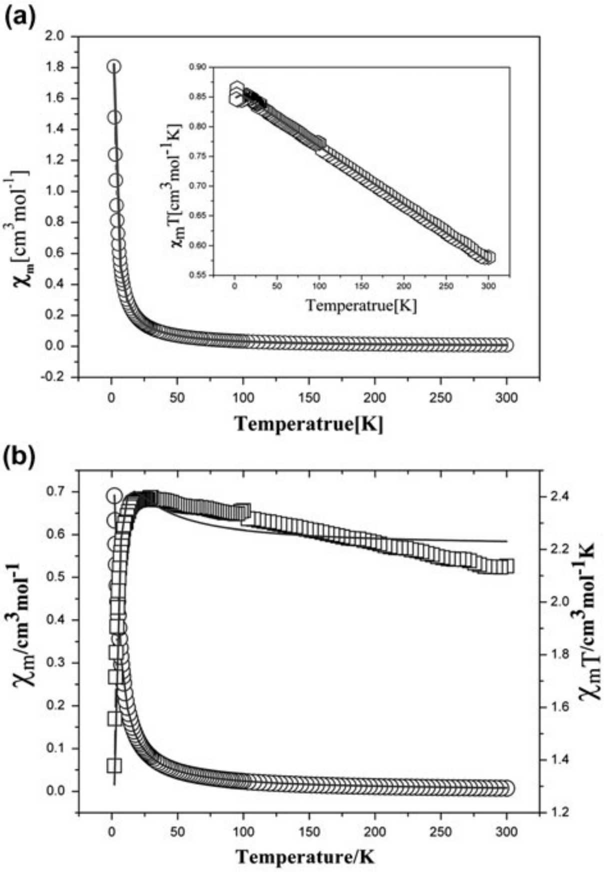

Figure 3. Temperature dependences of the magnetic susceptibilities of (a) **1** and (b) **2**. Solid lines represent the best fits.

where $\chi_M$ is the exchange-coupled magnetic susceptibility actually measured, $J$ is the exchange parameters between Cu(II) ions, and the rest of the parameters have their usual meanings. The best fit is obtained with values of $J = 0.027\ \mathrm{cm}^{-1}$, $g = 2.127$, and the agreement factor $R = 8.3 \times 10^{-7}$ ($R = \Sigma[(\chi_m)^{obs} - (\chi_m)^{calc}]^2/[(\chi_m)^{obs}]^2$), indicating a weak ferromagnetic interaction between Cu(II) ions, consistent with the magnetic behaviors illustrated by $\chi_m T$ *versus* $T$ plot in figure 3(a).

For **2**, the room temperature $\chi_m T$ value of $2.14\ \mathrm{cm^3\,K\,M^{-1}}$ is larger than the spin-only value of $1.00\ \mathrm{cm^3\,M^{-1}\,K}$ and is common for high-spin octahedral Ni(II) complexes ($S = 2/2$). Upon lowering the temperature, $\chi_m T$ smoothly increases until it reaches a maximum $\chi_m T$ value of $2.39\ \mathrm{cm^3\,K\,M^{-1}}$ around 26 K and then sharply diminishes to $1.38\ \mathrm{cm^3\,K\,M^{-1}}$ at 2 K, indicating weak ferromagnetic behavior from room temperature to 26 K, followed by ferromagnetic behavior below 26 K. Based on the spin Hamiltonian $H = -2JS_1S_2 (S_1 = S_2 = 1)$, the following equation was used to fit the magnetic susceptibility data (2):

$$\chi_M = \frac{2Ng^2\beta^2}{K(T-\theta)}\left[\frac{5+\exp(-4J/KT)}{5+3\exp(-4J/KT)+\exp(-6J/KT)}\right] \tag{2}$$

where $\chi_M$ is the exchange-coupled magnetic susceptibility actually measured, $J$ is the exchange parameters between Ni(II) ions, and the rest of the parameters have their usual meanings. The best fit is obtained with values of $J = 4.38\ \mathrm{cm}^{-1}$, $g = 1.62$, and $\theta = -3.18$ (agreement factor $R = 8.0 \times 10^{-7}$ ($R = \Sigma[(\chi_m)^{obs} - (\chi_m)^{calc}]^2/[(\chi_m)^{obs}]^2$)), indicating a weak ferromagnetic interaction between the Ni(II) ions, consistent with the magnetic behavior illustrated by $\chi_m T$ *versus* $T$ plot in figure 3(b).

## 4. Conclusion

Two germanium-substituted POM-supported transition metal complexes, $[Cu_2(phen)_4(GeW_{12}O_{40})]$ (**1**) and $[Ni_2(bpy)_4(H_2O)_2(GeW_{12}O_{40})]\cdot 2H_2O$ (**2**), were synthesized under hydrothermal conditions; the presence of $M(OH)_2$, $H_4GeW_{12}O_{40}\cdot nH_2O$, and phen(bpy) in the reaction system is essential for the formation of **1** and **2**. Cu(II) and Ni(II) are in **1** and **2**, respectively. For **2**, heteropolyanions $[GeW_{12}O_{40}]^{4-}$ are interconnected by two terminal oxygens of $[GeW_{12}O_{40}]^{4-}$ to form the POM-supported transition metal complex. Variable temperature magnetic measurements show an overall ferromagnetic behavior for **1** and a weak ferromagnetic behavior from 300 to 26 K followed by antiferromagnetic behavior below 26 K for **2**.

## Supplementary material

X-ray crystallographic files in CIF format for **1** and **2**; select bond distances, bond angles, and hydrogen bond parameters of **1** and **2**; IR spectra and TG/DTA curves of **1** and **2**. Crystallographic data for the two complexes in this paper have been deposited at the Cambridge Crystallographic Data Center, CCDC 953939 and 953959 for **1** and **2**, respectively. These data can be obtained free of charge at www.ccdc.cam.ac.uk/conts/retrieving.html [or from the Cambridge Crystallographic Data Center, 12 Union Road, Cambridge CB2 1EZ, UK; Fax: (+44) 1223/336-033; E-mail: deposit@ccdc.cam.ac.uk].

## Funding

This project was supported by the National Natural Science Foundation of China [grant number 51343003]; the Zhejiang Provincial Science and Technology Project of China [grant number 2011C31041]; the Scientific Research Fund of Zhejiang Provincial Education Department [grant number Y201224707], [grant number Y201120940].

## References

[1] (a) M.T. Pope. *Heteropoly and Isopoly Oxometalates*, Springer, Berlin (1983); (b) J.S. Anderson. *Nature*, **140**, 850 (1937); (c) H.T. Evans Jr. *J. Am. Chem. Soc.*, **70**, 1291 (1948).

[2] (a) C.L. Hill, C.M. Prosser-McCartha. *Coord. Chem. Rev.*, **143**, 407 (1995); (b) C.L. Hill. *Chem. Rev.*, **98**, 1 (1998); (c) U. Kortz, S.S. Hamzeh, N.A. Nasser. *Chem. Eur. J.*, **9**, 2945 (2003); (d) L.H. Bi, M. Reicke, U. Kortz, B. Keita, L. Nadjo, R.J. Clark. *Inorg. Chem.*, **43**, 3915 (2004); (e) B.B. Xu, Z.H. Peng, Y.G. Wei, D.R. Powell. *Chem. Commun.*, 2562 (2003).

[3] (a) A. Müller, S.Q.N. Shah, H. Bögge, M. Schmidtmann. *Nature*, **397**, 48 (1999); (b) L. Cronin, C. Beugholt, E. Krickemeyer, M. Schmidtmann, H. Bögge, P. Kögerler, T.K. Luong, A. Müller. *Angew. Chem. Int. Ed.*, **41**, 2805 (2002); (c) K. Fukaya, T. Yamase. *Angew. Chem. Int. Ed.*, **42**, 654 (2003); (d) X.K. Fang, T.M. Anderson, C. Benelli, C.L. Hill. *Chem. Eur. J.*, **11**, 712 (2005); (e) A. Müller, P. Kögerler, C. Kuhlmann. *Chem. Commun.*, 1347 (1999).

[4] (a) P. Mialane, A. Dolbecq, J. Marrot, E. Riviere, F. Secheresse. *Chem. Eur. J.*, **11**, 1771 (2005); (b) C.R. Mayer, C. Roch-Marchal, H. Lavanant, R. Thouvenot, N. Sellier, J.C. Blais, F. Secheresse. *Chem. Eur. J.*, **10**, 5517 (2004); (c) J.-H. Kang, J.A. Nelson, M. Lu, B.-H. Xie, Z.-H. Peng, D.R. Powell. *Inorg. Chem.*, **43**, 6408 (2004); (d) Z.H. Peng. *Angew. Chem. Int. Ed.*, **43**, 930 (2004).

[5] (a) C. Zhang, R.C. Howell, K.B. Scotland, F.G. Perez, L. Todaro, L.C. Francesconi. *Inorg. Chem.*, **43**, 7691 (2004); (b) L. San Felices, P. Vitoria, J.M. Gutiérrez-Zorrilla, S. Reinoso, J. Etxebarria, L. Lezama. *Chem. Eur. J.*, **10**, 5138 (2004).

[6] (a) S.S. Mal, U. Kortz. *Angew. Chem. Int. Ed.*, **44**, 3777 (2005); (b) U. Kortz, F. Hussain, M. Reicke. *Angew. Chem. Int. Ed.*, **44**, 3773 (2005); (c) B.S. Bassil, S. Nellutla, U. Kortz, A.C. Stowe, J. van Tol, N.S. Dalal, B. Keita, L. Nadjo. *Inorg. Chem.*, **44**, 2659 (2005); (d) F. Hussain, B.S. Bassil, L.-H. Bi, M. Reicke, U. Kortz. *Angew. Chem. Int. Ed.*, **43**, 3485 (2004); (e) U. Kortz, S. Nellutla, A.C. Stowe, N.S. Dalal, J. van Tol, B.S. Bassil. *Inorg. Chem.*, **43**, 144 (2004); (f) U. Kortz, S.S. Hamzeh, N.A. Nasser. *Chem. Eur. J.*, **9**, 2945 (2003); (g) F. Hussain, U. Kortz. *Chem. Commun.*, 1191 (2005).

[7] H.J. Pang, C.J. Zhang, J. Peng, Y.H. Wang, J.Q. Sha, A.X. Tian, P.P. Zhang, Y. Chen, M. Zhu. Z.M Su, *Eur. J. Inorg. Chem.*, **2009**, 5175 (2009).

[8] C.X. Li, R. Cao, K.P. O'Halloran, H.Y. Ma, L.Z. Wu. *Electrochim. Acta*, **54**, 484 (2008).

[9] F.X. Meng, J. Sun, K. Liu, F.X. Ma, Y.G. Chen. *J. Coord. Chem.*, **60**, 401 (2007).

[10] J.P. Wang, Y.Q. Feng, P.T. Ma, J.Y. Niu. *J. Coord. Chem.*, **62**, 1895 (2009).

[11] Y. Xu, J.Q. Xu, K.L. Zhang, Y. Zhang, X.Z. You. *Chem. Commun.*, 153 (2000).

[12] L.H. Bi, R.D. Huang, J. Peng, E.B. Wang, Y.H. Wang, C.W. Hu. *Dalton Trans.*, 121 (2001).

[13] G.Y. Luan, Y.G. Li, S.T. Wang, E.B. Wang, Z.B. Han, C.W. Hu, N.H. Hu, H.Q. Jia. *Dalton Trans.*, 233 (2003).

[14] J.P. Wang, Y.Q. Feng, P.T. Ma, J.Y. Niu. *J. Coord. Chem.*, **62**, 1895 (2009).

[15] B.B. Yan, Y. Xu, X.H. Bu, N.K. Goh, L.S. Chia, G.D. Stucky. *J. Chem. Soc., Dalton Trans.*, 2009 (2001).

[16] X.M. Zhang, B.Z. Shan, X.Z. You, Z.Y. Zhou, X.G. Zhou. *Polyhedron*, **16**, 713 (1997).

[17] Z.F. Li, B.S. Zhang, C.S. Wu. *Acta Crystallogr., Sect. E*, **65**, m741 (2009).

[18] Z.N. Jin, C.S. Wu, B.S. Zhang, W. Xu. *Z. Kristallogr. NCS*, **226**, 447 (2011).

[19] J.Q. Sha, L.J. Sun, E.L. Zheng, H.B. Qiu, M.Y. Liu, H. Zhao, H. Yuan. *J. Coord. Chem.*, **66**, 602 (2013).

[20] X.L. Wang, C. Xu, H.Y. Lin, G.C. Liu, J. Luan, Z.H. Chang, A.X. Tian. *J. Coord. Chem.*, **66**, 1451 (2013).

[21] S.H. Yang, X.Q. Dong, Y.P. Zhang, H.M. Hu, G.L. Xue. *J. Coord. Chem.*, **66**, 1529 (2013).

[22] J. Wu, Y.L. Xu, K. Yu, Z.H. Su, B.B. Zhou. *J. Coord. Chem.*, **66**, 2821 (2013).

[23] X. Gan, X.X. Hu, Z.F. Shi, Y.Z. Yin. *J. Coord. Chem.*, **66**, 2930 (2013).

[24] R. Yang, S.X. Liu, Q. Tang, S.J. Li, D.D. Liang. *J. Coord. Chem.*, **65**, 891 (2012).

[25] H.B. Liu, Y. Sun, Y.G. Chen, F.X. Meng, D.M. Shi. *J. Coord. Chem.*, **61**, 3102 (2008).

[26] Y.B. Liu, Y. Wang, L.N. Xiao, Y.Y. Hu, L.M. Wang, X.B. Cui, J.Q. Xu. *J. Coord. Chem.*, **65**, 4342 (2012).

[27] J.Y. Niu, Q.X. Han, J.P. Wang. *J. Coord. Chem.*, **56**, 523 (2003).

[28] J. Wu, C.X. Wang, K. Yu, Z.H. Su, Y. Yu, Y.L. Xu, B.B. Zhou. *J. Coord. Chem.*, **65**, 69 (2012).

[29] A.X. Tian, X.L. Lin, Y.J. Liu, G.Y. Liu, J. Ying, X.L. Wang, H.Y. Lin. *J. Coord. Chem.*, **65**, 2147 (2012).

[30] C. Rocchiccioli-Deltcheff, M. Fournier, R. Franck, R. Thouvenot. *Inorg. Chem.*, **22**, 207 (1983).

[31] G.M. Sheldrick. *Acta Crystallogr. Sect. A*, **64**, 112 (2008).

[32] R. Thouvenot. *Spectrosc. Lett.*, **12**, 127 (1979).